Stress-Induced Characteristics of Silicon-on-Insulator Rib Waveguides

M. M. Milošević, P. S. Matavulj, *Member IEEE,* and G. Z. Mashanovich

***Abstract* — In this paper the influence of stress induced effect in the most popular Silicon-on-Insulator (SOI) small rib waveguide is analysed. Birefringence-free condition and the influence of the top oxide cladding are investigated and appropriate design rules for this type of SOI waveguides are presented.**

***Keywords* — Birefringence, polarization, silicon photonics, stress, waveguide.**

I. Introduction

RECENT years have seen an enormous increase in bandwidth requirements for telecom and datacom transmission systems. This has put stronger demands for increased functionality, reduced cost and full integration of photonic components that are necessary to provide all ever-increasing demands. These requests can be achieved by using high-index-contrast material system, such as silicon-on-insulator (SOI). Although the SOI platform was first reported in 1989 it became today the most popular choice for waveguide systems [1], [2]. The research in silicon started with planar waveguides [3] and continued with large rib waveguides [4]. Recently a lot effort has been made for making low cost and compact integrated photonic devices and that's why both rib [5] and strip waveguides [6] have been intensively investigated. Typical wavelengths for SOI applications are 1.33μm and 1.5μm, but longer wavelengths are not suitable (except in the 3–3.5μm range) due to absorption spectra in silicon dioxide [7]. There are several areas like sensing, communications, signal processing and imaging where this platform can find valuable application.

In an SOI waveguide, light is guided in a silicon core separated from the silicon substrate by a buried SiO_2 layer (BOX) acting as the lower cladding. High index contrast between the cladding and waveguide core facilitates the optical confinement and guiding of light. The design rules for small rib waveguides (1.0μm<H<1.5μm) have been reported, but only with air top cladding [5]. The influence of the top oxide cover has been analysed for larger rib waveguides with height of 2.2μm [8]. In this paper, the influence of the top oxide cover on polarization characteristics of a SOI rib waveguide with H=1.3μm has been analysed. It will be shown that the top oxide cover need to be analysed when calculating the birefringence and that the stress engineering represents very important tool to control, modify and achieve polarization independent SOI waveguides that is nowadays highly desirable.

The paper is organized as follows. In Sec. II. the stress theory and its influence to the total birefringence is presented. The obtained results are discussed in Sec. III, while the concluding remarks are summarized in Sec. IV.

M. M. Milošević and P. M. Matavulj are with the Faculty of Electrical Engineering, University of Belgrade, Bulevar kralja Aleksandra 73, 11120 Belgrade, Serbia; (phone: +381 11 3370 155, fax: +381 11 3248 681, e-mail: milance24@gmail.com; matavulj@etf.bg.ac.yu).

G. Z. Mashanovich is with the Advanced Technology Institute, School of Electronics and Physical Sciences, University of Surrey, Guildford, GU2 7XH, UK; (e-mail: g.mashanovich@surrey.ac.uk).

II. Waveguide Stress Theory

Modal waveguide birefringence is defined here as the difference between the effective indexes of the two orthogonally polarized modes, horizontally polarized mode (quasi-TE) and vertically polarized mode (quasi-TM) $\Delta N_{eff} = N_{eff}^{TE} - N_{eff}^{TM}$. To achieve zero-birefringence, an optimisation of rib waveguide dimensions is necessary [5]. The total birefringence is, however, the sum of the geometrical birefringence (ΔN_{geo}) and stress induced birefringence (ΔN_{stress}) [8]: $\Delta N_{eff} = \Delta N_{geo} + \Delta N_{stress}$. The Scanning Electron Microscope (SEM) cross section view of an SOI waveguide is given in Fig. 1. (a), while the Fig. 1 (b) shows the geometry of modelled rib waveguide. The stress in the upper SiO_2 layer produces a stress distribution within and near the Si rib, which in turn causes a change of the refractive index in both materials due to the photoelastic effect. We assume that the thickness of the upper cladding film on the rib sidewalls is 70% of that on the top to simulate the film deposition used in experiments. The stress induced birefringence can be expressed as

$$\begin{aligned} \Delta N_x &= N_x - N_0 = -C_1\sigma_x - C_2(\sigma_y + \sigma_z) \\ \Delta N_y &= N_y - N_0 = -C_1\sigma_y - C_2(\sigma_x + \sigma_z). \end{aligned} \quad (1)$$

Here, σ_x, σ_y and σ_z are the principal components of the relative stress tensor, N_x and N_y are the components of the material's refractive index, N_0 is the refractive index without stress, and C_1 and C_2 are the stress-optic constants related to the Young's modulus (E), Poisson's ratio (ν), and the photoelastic tensor elements (p_{11} and p_{12}) as

$$\begin{aligned} C_1 &= \frac{N^3}{2E}(p_{11} - 2\nu p_{12}) \\ C_2 &= \frac{N^3}{2E}(-\nu p_{11} + (1-\nu)p_{12}) \end{aligned} \quad (2)$$

In this paper, an operating wavelength of λ=1.55μm is considered. One source of birefringence, however, is strain due to the temperature difference before and after manufacturing processes (between the operating

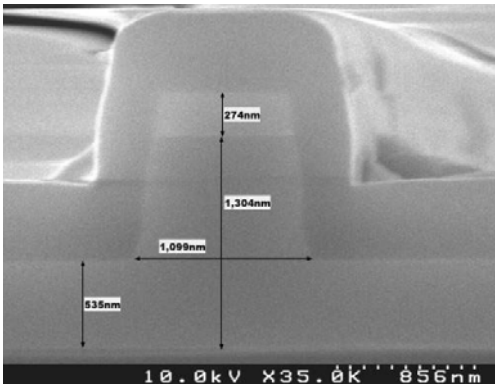

(a)

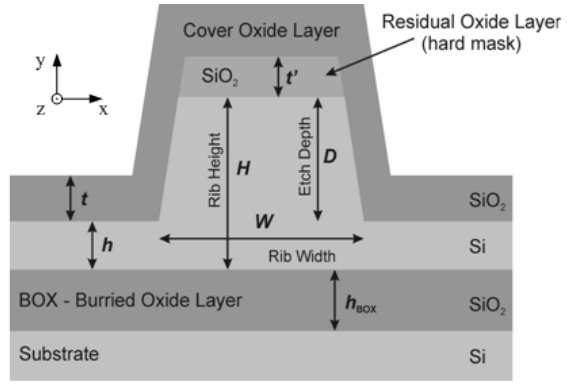

(b)

Fig. 1. Rib waveguide cross-section view (a) SEM srtucture; (b) modelled structure (t is the top oxide layer thickness, H is rib height, D (D=H-h) is etch depth and W is waveguide rib width).

temperature T_0 and film deposition temperature T_{ref}: $\Delta T=T_0-T_{ref}$). The stress and strain are related as follows:

$$\begin{bmatrix}\varepsilon_x\\ \varepsilon_y\\ \varepsilon_z\end{bmatrix}=\frac{1}{E}\begin{bmatrix}1 & -\nu & -\nu\\ -\nu & 1 & -\nu\\ -\nu & -\nu & 1\end{bmatrix}\begin{bmatrix}\sigma_x\\ \sigma_y\\ \sigma_z\end{bmatrix}+\alpha\Delta T\cdot I, \quad (3)$$

where ε_x, ε_y, and ε_z are the principal strain components along the x, y and z direction, respectively, α is thermal expansion coefficient and I is the unit matrix. As it can be seen from the Eq. 3 the stress consists of the photoelastic strain and thermal induced strain. By inverting Eq. 3 the stress distribution can be obtained and further, according to Eq. 1 the material refractive index distribution. Now, we can solve Maxwell's equations

$$\nabla\times\varepsilon_r^{-1}\times\overrightarrow{H}=k_0^2\overrightarrow{H}, \quad (4)$$

where $\varepsilon_r=N^2$ and $k_0=\frac{2\pi}{\lambda}$. The simulation was set up with normalized magnetic field components $\overrightarrow{H}=(H_x,H_y,H_z)$ as dependent variables. The wave is assumed to travel in z direction and has the form

$$\overrightarrow{H}=\overrightarrow{H}(x,y)e^{j(\omega t-\beta z)}. \quad (5)$$

The effective mode index $N_{eff}=\beta/k_0$ is obtained from eigenvalues.

The stress influence in the waveguide and Maxwell's equations are solved by the finite element method (FEM), on a nonuniform mesh of triangular elements. For our numerical computations, approximately 40000 elements and the higher order shape functions of Lagrange type are used.

III. Numerical Results and Discussion

The rib waveguide analysed in this paper has a buried oxide (BOX) layer of 1µm in thickness, rib width of 1.099µm, height of 1.304µm, and etch depth of 0.769µm (Fig 1 a)). The stress in the upper SiO_2 layer produces a stress distribution within and near the Si rib, which in turn causes a change of the refractive index in both materials due to the photoelastic effect. Assumed thickness of the upper cladding film on the rib sidewalls is 70% of that on the top (Fig. 1 b)). There is additional oxide layer, the hard mask used during the etching of the rib. Its thickness is 0.274µm. Sidewall angle is assumed to be 8 degrees. The refractive indices, at the wavelength of 1550nm, for the

Table 1: Material parameters used in the calculations for wavelength of 1550 nm

Material	Photoelastic tensor elements		Youngs Modulus (GPa)	Poissons ratio
	p_{11}	p_{12}		
Si	-0.101	0.0094	130	0.27
SiO_2	0.16	0.27	76.7	0.186

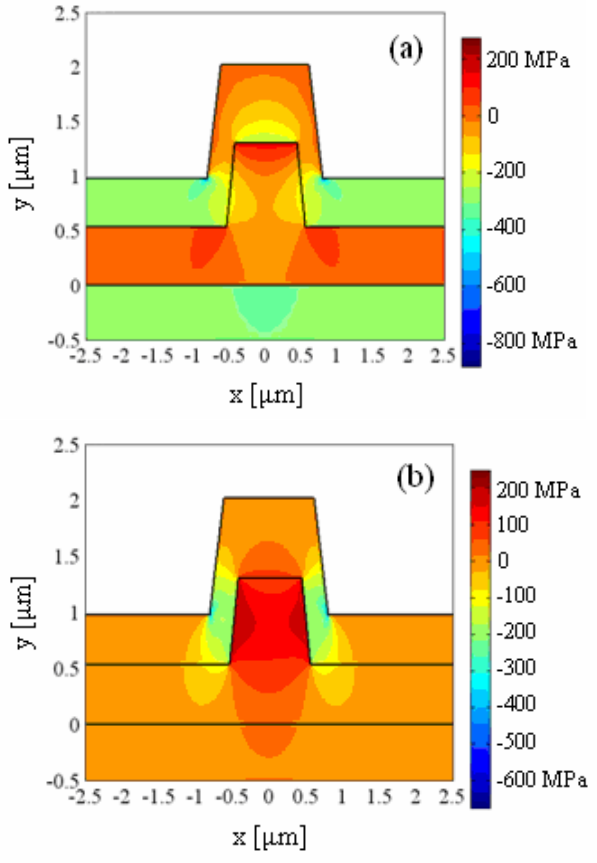

Fig. 2. Stress field distribution a) in the x direction, σ_x and b) in the y direction, σ_y.

silicon guiding layer and SiO_2 used in the model are 3.476 and 1.444, respectively. The thermal expansion coefficients for Si and SiO_2 layers are 3.6×10^{-6} K^{-1} and 5.4×10^{-7} K^{-1}, whilst the difference between the operating and reference temperature is assumed to be -980 K. Other

parameters used in calculations are given in Table 1.

Fig. 2 shows the simulated stress distribution in x and y direction of waveguide cross section. It is worth mention that we assumed that strain component along the propagation z direction is negligible compared to the strain components in x and y directions. This provide good enough accuracy and calculation time. Computation window size for stress calculation is set to be 100μm×100μm, large-wide enough that the edge effects do not distort the stress distribution in the vicinity of the ridge waveguide. At the waveguide center, we get $\sigma_x \approx$ -66MPa, $\sigma_y \approx$ 124MPa, while for SiO_2 upper and lower cladding $\sigma_{film} \approx$ -290MPa (σ_{film} represents the in-plane stress component in the uniform film far enough from the ridge). The primarily in-plane (x) stress in the oxide film compresses Si ridge resulting in a compressive strain in the x direction and higher tensile strain in the y direction. This anisotropy is the main reason for stress-induced birefringence.

Fig. 3 and Fig. 4 show the anisotropy of the refractive index in the middle of the core in SOI waveguide. For a given y value (y=0.652μm) in the middle of the waveguide core (Fig. 3) change in the refractive index of Si is symmetric, what is expected, and far enough from the center of the core it is constant. This fact is according to

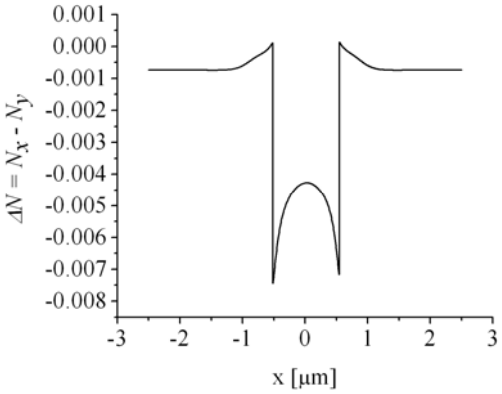

Fig. 3. Refractive index change in the x direction in the middle of the core in SOI rib waveguide

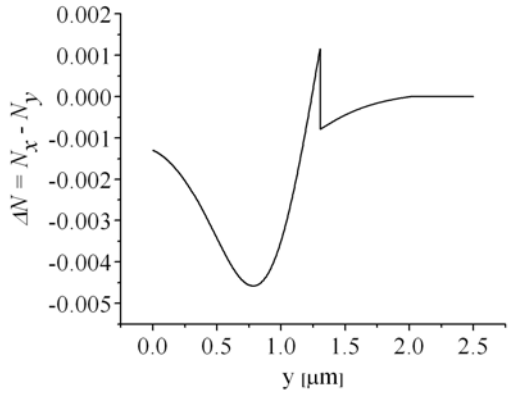

Fig. 4. Refractive index change in the y direction in the middle of the core in SOI rib waveguide

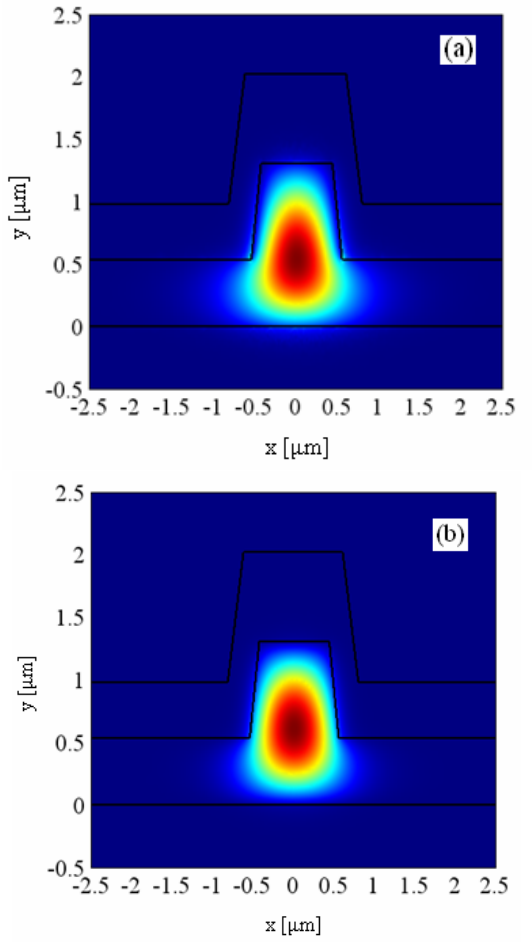

Fig. 5. Field profiles for a) quasi-TE mode and b) quasi-TM mode

the stress distribution in the x and y direction (Fig. 1 a) and Fig. 1 b)) far enough from the waveguide center where the stress value is practically constant ($\sigma_{film} \approx$ -290MPa; $\sigma_y \approx$ 0.014MPa). Similar to this is the case when y coordinate is varied for a given x (x=0) in the waveguide core center (Fig 4). It can be seen that the curve of the materials refractive index change approaches to zero (isotropic case) when y is higher then 2μm. This value is just above the top of the upper oxide cover and because there is no stress influence the anisotropy of the refractive index vanishes.

The results of optical mode analysis are given in Fig. 5. Here, the computation domain was reduced significantly, because the energy of the fundamental modes is concentrated in the core region, and the energy density primarily decays rapidly in the top oxide cladding and BOX region. The increased polarization dependence in small rib waveguides is derived from the increasingly differing mode shapes of the quasi-TE and quasi-TM modes. We use ‘quasi-TE’ and ‘quasi-TM’ terms because there are no pure TE and TM modes in strip and rib waveguides.

Fig. 6 shows the influence of the top oxide cover on the birefringence. For air cover, the total birefringence is equal to the geometrical birefringence and it is positive. The oxide cover reduces the total birefringence and for thick oxides it becomes negative. The effective indices of

the fundamental quasi-TE and quasi-TM modes without stress influence are shown in the Fig. 6 a).

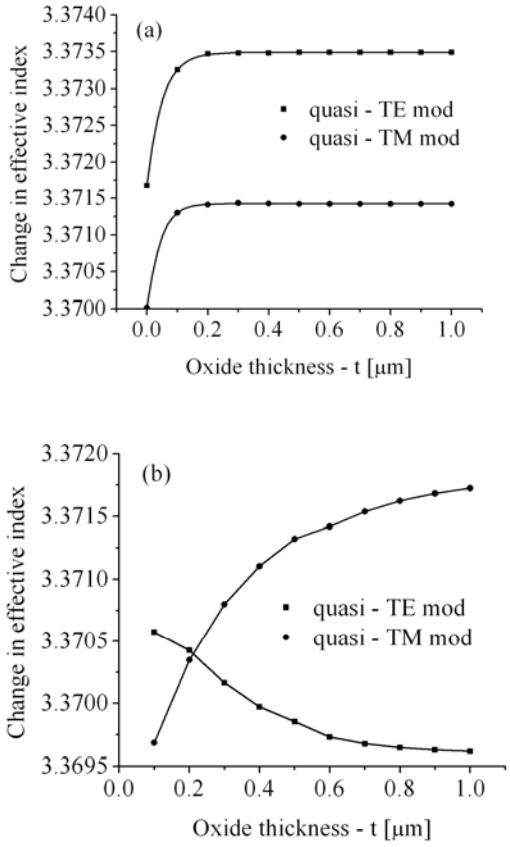

Fig. 6. Changes in the effective index as a function of the top oxide cover thickness in SOI rib waveguide a) without stress ($\sigma_{film} = 0$) and b) when stress effects are taken into account ($\sigma_{film} \approx$ -290 MPa).

In the presence of thin oxide cover mode confinement is slightly reduced. A finite fraction of optical energy penetrates in the oxide and both fundamental modes become higher. For an oxide cover of 0.3μm both curves saturate and zero birefringence condition is not achieved. When top oxide cover is under compressive stress material indexes will change (Fig. 3 and Fig. 4) causing the corresponding changes in the modal effective indices (Fig. 6 b)). As said previously, the stress is mainly governed by the cover oxide because the lower BOX layer exerts little force on the Si ridge due to the plane interference between the BOX layer and the core. As shown in the Fig. 6 b) N_{eff}^{TE} decreases with the oxide thickness increase, while N_{eff}^{TM} increases. The absolute values of change are larger for TM mode than that for TE mode and curves will saturate for large values of top oxide cover thickness.

It can be seen that for the oxide thickness of ~220nm zero-birefringence can be achieved. Therefore, by stress engineering, zero-birefringence can be achieved for a waveguide that has otherwise relatively large birefringence.

IV. Conclusion

High index contrast waveguide platforms such as SOI opens new opportunities for integrated, high-functionality photonic circuits for applications in data transmission, telecommunication and optical analysis. In this paper we have presented the characteristic of the geometrical and stress-induced birefringence for SOI rib waveguide with height of 1.3μm. We have examined design guidelines for conventional SOI rib waveguides which are the most common structures for near infrared silicon photonic applications. It has been shown that by stress engineering, zero-birefringence can be achieved for a waveguide that has otherwise relatively large birefringence.

References

[1] E. Cortesi, F. Namavar, and R. A. Soref, "Novel silicon-on-insulator structures for silicon waveguides," in *Proc. IEEE SOS/SOI Tech. Conf. (Cat. No.89CH2796-1),* Stateline, NV, USA, Oct. 1989, pp. 109.

[2] B. N. Kurdi and D. G. Hall, "Optical waveguides in oxygen-implanted buried-oxide silicon-on-insulator structures," *Opt. Lett.,* vol. 13, no. 2, pp. 175-177, Feb. 1988.

[3] A. Rickman, G. T. Reed, B. L. Weiss, and F. Namavar, "Low-loss planar optical waveguides fabricated in SIMOX material," *IEEE Photon. Tech. Lett.*, vol. 4, no. 6, pp. 633-635, June 1992.

[4] J. Schmidtchen, A. Splett, B. Schuppert, and K. Petermann, "Low loss integrated-optical rib-waveguides in SOI," in *1991 Proc. IEEE International SOI Conf.* (Cat. No.91CH3053-6), pp. 142-143.

[5] S. P. Chan, C. E. Png, S. T. Lim, V. M. N. Passaro, and G. T. Reed, "Single mode and polarisation independent SOI waveguides with small cross section," *J. Lightwave Tech.*, vol. 23, no. 6, pp. 1573-1582, June 2005.

[6] K. Yamada, H. Fukuda, T. Watanabe, T. Tsuchizawa, T. Shoji, and S.-I. Itabashi, "Functional photonic devices on silicon wire waveguide," in *Proc. LEOS 2nd Group IV Photonics*, Antwerp, Belgium, Sept. 2005, pp. 186-188.

[7] R. A. Soref, S. J. Emelett, and W. R. Buchwald, "Silicon waveguided components for the long-wave infrared region," *J. Opt. A: Pure Appl. Opt.*, vol. 8, no. 10, pp. 840-848, July 2006.

[8] W. N. Ye, D.-X. Xu, S. Janz, P. Cheben, M.-J. Picard, B. Lamontagne, and N. G. Tarr, "Birefringence control using stress engineering in silicon-on-insulator (SOI) waveguides," *J. Lightwave Technol.*, vol. 23, no. 3, pp. 1308-1318, Mar. 2005.

[9] M. Huang, "Stress effects on the performance of optical waveguides," *Int. J. Sol. Structures*, vol. 40, no. 7, pp. 1615-1632, Apr. 2003.

[10] L. Vivien, S. Laval, B. Dumont, S. Lardenois, A. Koster, and E. Cassan, "Polarization-independent single-mode rib waveguides on silicon-on-insulator for telecommunication wavelengths," *Opt. Commun.*, vol. 210, pp. 43-49, no. 1-2, Sept. 2002.